# MICRO-MECHANICS OF FRACTURE AND FAILURE OF GEO-MATERIALS IN COMPRESSION

**S. Nemat-Nasser and H. Horii**

*Department of Civil Engineering, The Technological Institute, Northwestern University, Evanston, IL 60201, USA*

ABSTRACT

Recent analytical results on non-coplanar crack growth in elastic solids under far-field compressive stresses, are used to examine the micro-mechanics of brittle failure in compression. The three distinct failure modes -- axial splitting, faulting, and the transition from brittle to ductile response -- observed under axial compression for different confining pressures, are discussed in terms of simple plausible micro-mechanical models. The failure strength and the orientation of failure planes, as well as the stress ratio which marks the brittle-ductile transition, are estimated and compared with published data on various rocks, arriving at good correlations. In addition, certain model experiments which seem to support the analytical models, are examined.

KEY WORDS

Micro-cracks; Mechanisms of failure; Analytical models; Model experiments

## 1. INTRODUCTION

At suitably low temperatures where rate-effects may be regarded insignificant, the inelastic response of brittle solids to a large extent stems from the formation of micro-cracks at grain boundaries, at interfaces between dissimilar grains, at pre-existing voids, and at other flaws or inhomogeneities. Under overall compressive forces, the nucleation and growth of micro-cracks are accompanied by local plastic deformation of soft inhomogeneities, cleavage of suitably oriented inclusions, and frictional sliding of pre-existing flaws or a set of grain boundary cavities; see, for example, Olsson and Peng (1976), Tapponnier and Brace (1976), Wong (1982), and Paterson (1978) for a discussion. These comments apply to rocks, concrete, and even some brittle metallic composites at suitably low temperatures. The response and the failure mechanism of these materials under far-field compressive forces are quite different from their behavior under far-field tensile forces.

The purpose of this note is to briefly outline some recent work on compression-induced, non-coplanar growth of cracks in elastic solids containing pre-existing flaws, and to relate these results to the problem of failure of brittle solids with micro-structure under far-field compressive forces.

The physical phenomena of concern here are the three distinct failure modes observed when, for example, a sample of rock (e.g. marble, granite, or sandstone) is axially compressed under different lateral confining pressures. It is well known that, in the absence of any confining pressures, the sample fails by axial splitting along fracture planes which run parallel to the direction of compression; this is called axial splitting. When some lateral compression also exists, then the sample fails by faulting along a plane inclined with respect to the axial compression. When the confining pressure is suitably large, e.g. greater than 25-30% of the peak axial stress, then the sample undergoes plastic deformation and behaves essentially like ductile metals. Indeed, under suitable overall uniform compression, a cylindrical sample of rock will neck like mild steel, when subjected to additional lateral pressures, or it will deform into a barrel-shape when subjected to additional axial compression. In Fig. 1 these three failure modes are shown for marble samples.

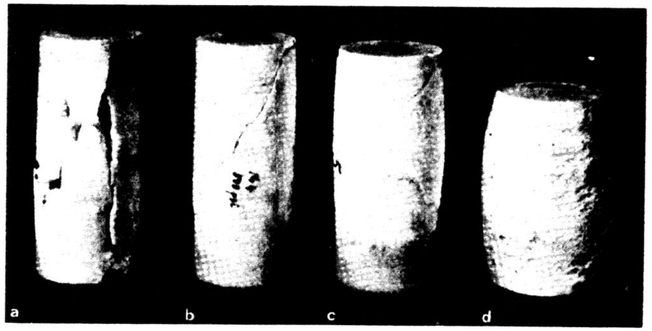


Fig. 1. Types of fractures or flow in Wombeyan marble at various confining pressures: (a) axial splitting failure at atmospheric pressure; (b) single shear failure at 3.5 MPa (35 bars); (c) conjugate shears at 35 MPa (350 bars); (d) ductile behaviour at 100 MPa (1kbar). (From Paterson, 1978)

## 2. AXIAL SPLITTING

Various models have been proposed in the literature, in order to explain the micro-mechanical processes that are responsible for axial splitting. For example Brace and Bombolakis (1963) and Hoek and Bieniawski (1965) performed experiments on glass plates containing pre-existing cracks, showing that under axial compression, the pre-existing cracks would kink, growing out of their plane and curving toward the axial compression. Recently, Nemat-Nasser and Horii (1982) gave an analytic solution of this problem and showed that crack growth of this kind can become unstable if some (possibly quite small) lateral tension accompanies axial compression. On the other hand, out-of-plane crack growth will be arrested if some lateral compression is present.



Figure 2 shows the considered elasticity boundary-value problem; Nemat-Nasser and Horii (1982), Nemat-Nasser (1983), and Horii and Nemat-Nasser (1983). On the pre-existing flaw PP', we require that

$$u_y^+ = u_y^-, \quad \tau_{xy}^+ = \tau_{xy}^- = -\tau_c + \mu\sigma_y, \tag{1}$$

and on the curved cracks PQ and P'Q', we have

$$\sigma_\theta = \tau_{r\theta} = 0, \tag{2}$$

where $\tau_c$ is the cohesive (or yield) stress, $\mu$ is the frictional coefficient, $u_y$ is the displacement in the y-direction, $\sigma_y$ is the normal stress and $\tau_{xy}$ is the shear stress on PP', and $\sigma_\theta$ is the hoop stress and $\tau_{r\theta}$ is the shear stress on PQ. Superscripts + and - denote the value of the considered quantities above and below the x-axis.

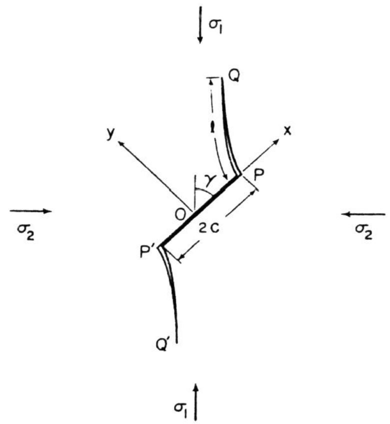


Fig. 2. Pre-existing flaw PP' and curved tension cracks PQ and P'Q'.

Figure 3 shows some typical results. As is seen, in the presence of small lateral tension, crack growth becomes unstable after a certain crack extension length is attained. This unstable crack growth is considered to be the fundamental mechanism of axial splitting of a uniaxially compressed rock specimen. Peng and Johnson (1972) report the presence of lateral tension in the uniaxially compressed specimen because of the end-boundary conditions. Different inserts affect the ultimate strength: the strength, measured by the peak value of $|\sigma_1|\sqrt{\pi c}/K_c$, is 9.5 for the steel insert, 7.3 for the teflon insert, and 5.9 for the neoprene insert; here $K_c$ is the fracture toughness in Mode I. They also report a radial tensile stress of 6-8% of applied compression for the neoprene insert, and 4-6% for the teflon insert. These experimental data seem to support our analytical results.

Nemat-Nasser and Horii (1982) have made a series of model experiments and have shown that unstable growth of tension cracks discussed above, may indeed be the basic micro-mechanism of axial splitting; see their Figs. 13-20.

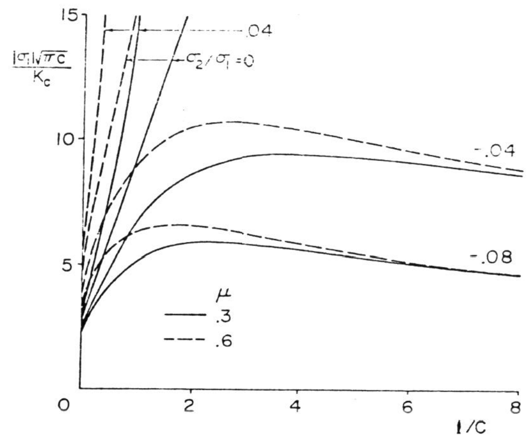


Fig. 3. Normalized axial compression required to attain the associated crack extension length; Horii and Nemat-Nasser (1983).

## 3. FAULTING

In the presence of a confining pressure, an axially compressed sample of rock fails by faulting or (macroscopic) shear failure. To explain the mechanics of such faulting, some authors have emphasized the role of Euler-type buckling associated with columnar regions formed in the sample because of axial cracking; see, for example, Fairhurst and Cook (1966), Janach (1977), and Holzhausen and Johnson (1979).

A different model has been suggested by Horii and Nemat-Nasser (1983). This model considers a row of suitably oriented micro-flaws and seeks to estimate the axial compression at which out-of-plane cracks that nucleate from the tips of these flaws can suddenly grow in an unstable manner, leading to the formation of a fault; see Fig. 4. The solution of the elasticity problem associated with a solid containing a row of periodically distributed flaws with out-of-plane micro-cracks, is given by Horii and Nemat-Nasser (1983). Typical results are shown in Fig. 5. For small values of $\phi$, the axial compression first increases with increasing crack extension length, attains a peak value, decreases, and then begins to rise again. This suggests an unstable crack growth at a critical value of the axial stress, which may lead to the formation of a fault zone. It is seen from Fig. 5 that the peak values of the axial stress for the values of $\phi$ from $0.16\pi$ to $0.2\pi$ fall in a very narrow range, i.e. $|\Delta\sigma_1|\sqrt{\pi c}/K_c \sim 0.3$. This implies that the overall failure angle is sensitive to imperfection and other effects. Indeed, the orientation of the fracture plane observed in experiments often scatters over a certain range. The range of the overall failure angle, however, may be limited since the peak value of the axial stress increases sharply as $\phi$ decreases. We can specify the possible range of the overall orientation angle $\phi$ by prescribing the "stress barrier" $|\Delta\sigma_1|\sqrt{\pi c}/K_c$ which can be overcome. Note that the value of $\gamma$ in Fig. 4 is chosen such that the required axial compression for instability is minimized.



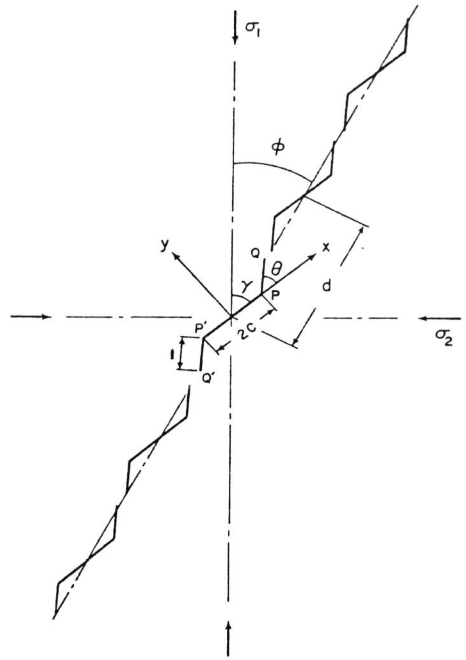


Fig. 4. An infinite plate with a row of pre-existing flaws and tension cracks at their tips.

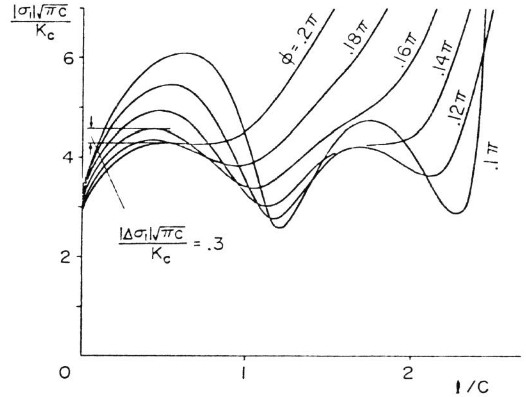


Fig. 5. Axial stress versus crack extension length: $\gamma = 0.24\pi$, $\tau_c = 0$, and $\mu = 0.4$; Horii and Nemat-Nasser (1983).

Now one can calculate the critical axial load, $|\sigma_1|\sqrt{\pi c}/K_c$, and the possible range of the overall failure angle, $\phi$, for a given confining pressure and flaw spacing d/c. In the actual rock specimen, there are many flaws of various sizes. It is reasonable to expect that smaller flaws are greater in number and closer in spacing. Thus, one may assume that the spacing of the "optimally oriented" flaws is an increasing function of the flaw size. For illustration, we introduce the simple relation,

$$d/c_m = b(c/c_m)^{1+a}, \quad b = d_m/c_m, \quad a > 0, \tag{3}$$

where $c_m$ and $d_m$ denote the minimum flaw size and the corresponding flaw spacing, and a is a constant. With this relation we can calculate the ultimate strength (i.e. the minimum axial critical load) and the possible range of the overall failure angle as functions of the confining pressure. Typical results are shown in Figs. 6a,b with $d_m/c_m$ = 3.0, a = 0.18, and $K_c/\sqrt{\pi c_m}$ = $8\times10^3$ psi. The corresponding experimental data on Darley Dale sandstone reported by Murrell (1965) are also shown in these figures.

Horii and Nemat-Nasser (1983) report results of a series of model experiments designed specifically to bring out the influence of lateral compression on the mechanism of crack growth under axial compression; see their Figs. 2,3,9,10,19, and 20.

It should be emphasized that the out-of-plane cracks observed to grow from the tips of flaws in experiments reported by Horii and Nemat-Nasser, are tension cracks, even though the sample is under rather large overall compressive forces (i.e. all three far-field overall principal stresses are compressive). Indeed, when the lateral confining pressure is rather small, it is easy to show by model experiments of the kind reported by Nemat-Nasser and Horii (1982), see their Figs. 17-20, that pre-existing frictional cracks cannot extend in Mode II (i.e. shear mode), no matter what the orientation, size, and distribution of these pre-existing cracks may be.

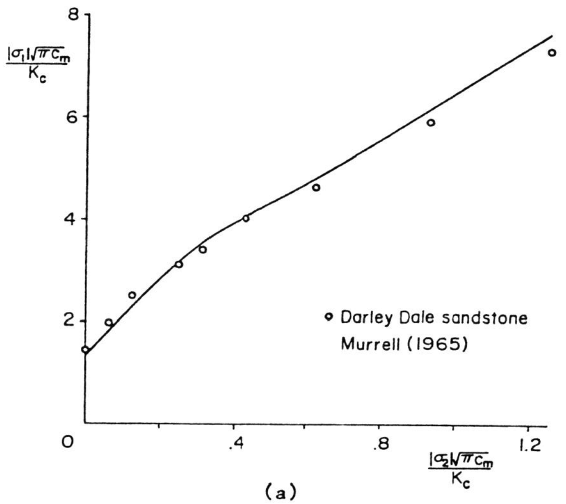


(a)



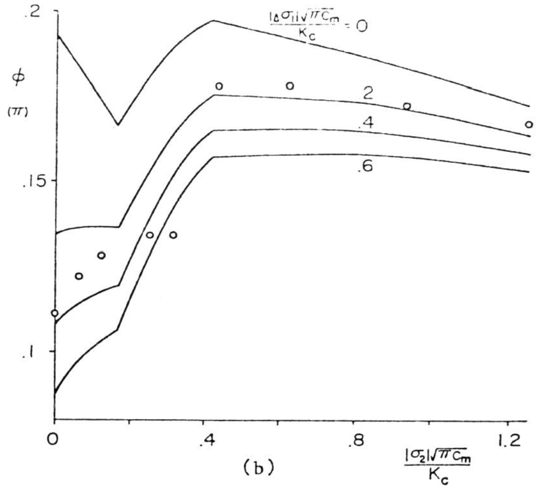


(b)

Fig. 6. Variations of (a) the ultimate strength, and (b) the overall failure angle with the confining pressure; Horii and Nemat-Nasser (1983).

## 4. BRITTLE-DUCTILE TRANSITION

A dramatic change in the mechanism of crack growth occurs, once the lateral compression is sufficiently large. When the confining pressure is still below the brittle-ductile transition value, out-of-plane tension cracks are still nucleated from the flaws. However, if the lateral confinement is large enough, the growth of these tension cracks is suppressed. Moreover, the instability observed in simultaneous growth of out-of-plane tension cracks from the tips of a row of pre-existing flaws is also suppressed by large enough lateral confining pressures. Nemat-Nasser and Horii (1983) show that then a plastic zone begins to develop at the tips of the pre-existing flaws and, indeed, the flaws tend to extend in Mode II by in-plane plastic sliding, accompanied by the formation of out-of-plane tension cracks, which cracks curve toward the axial compression.

Figure 7 shows the considered model, where $\ell_t$ and $\ell_p$ are the length of the tension crack and the size of the plastic zone, respectively. For the flaw, PP', and the cracks, PQ and P'Q', the boundary conditions are given by Eqs. (1) and (2), respectively. Across the plastic zones, PR and P'R', we require,

$$u_y^+ = u_y^-, \quad \tau_{xy} = -\tau_Y, \tag{4}$$

where $\tau_Y$ is the yield stress in shear (assumed to be a constant in the following results).

For given stress ratio, $\sigma_2/\sigma_1$, Fig. 8 shows the graphs of $\ell_p/c$ vs $\ell_t/c$, for $K_c/\tau_Y\sqrt{\pi c}$ = 0.04; this nondimensional parameter represents the overall ductility of the solid. It is seen that for small lateral compressions, $\ell_p/c$

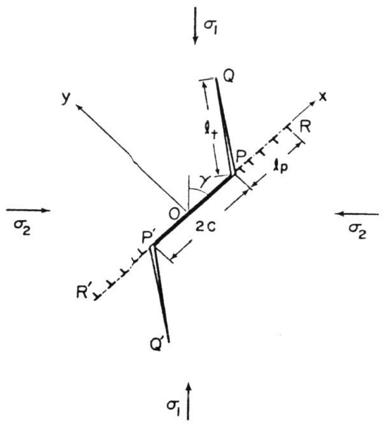


Fig. 7. Straight cracks PQ and P'Q' and plastic zones PR and P'R' at the tips of a pre-existing flaw PP'.

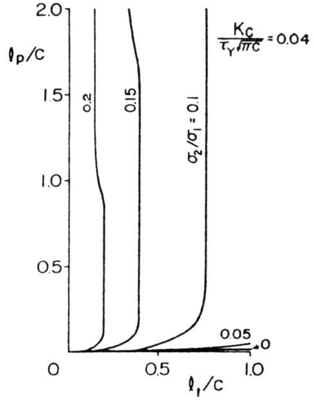


Fig. 8. Relations between crack length and plastic zone size: $\gamma = 0.25\pi$, $\tau_c = 0$, and $\mu = 0.4$.

remains very small as $\ell_t/c$ increases; the solid is "brittle" in this case. With suitably large values of $\sigma_2/\sigma_1$, on the other hand, $\ell_t/c$ ceases to increase after it attains a certain value, while $\ell_p/c$ continues to increase with increasing axial compression. Indeed, for large enough $\sigma_2/\sigma_1$ (i.e. $\sigma_2/\sigma_1 = 0.2$), the tension crack actually begins to relax and close as the plastic zone extends. We suggest that this may be the fundamental mechanism responsible for the brittle-ductile transition. In fact, if the peak values of $\ell_t/c$ (denoted by $(\ell_t/c)_{max}$) are plotted against $\sigma_2/\sigma_1$, Fig. 9 is



obtained. For $\sigma_2/\sigma_1$ exceeding 0.2 to 0.25, this figure shows a transition to the ductile response. This is in accord with experimental observations; Mogi (1966).

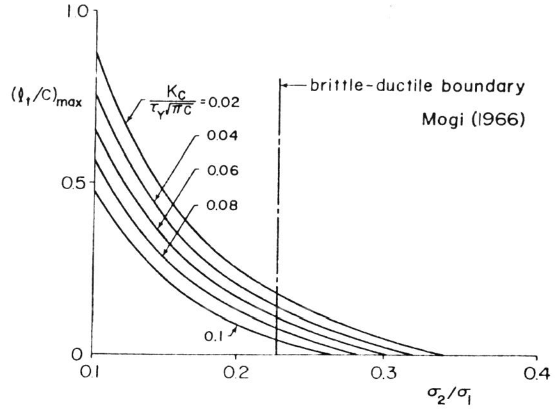


Fig. 9. The maximum length of tension cracks as a function of stress ratio.


ACKNOWLEDGMENT

This work has been supported by the U.S. Air Force Office of Scientific Research grant AFOSR-84-0004 to Northwestern University.


REFERENCES


Brace, W. F., and E. G. Bombolakis (1963). A note on brittle crack growth in compression. J. Geophys. Res., 68(12), 3709-3713.

Fairhurst, C., and N. G. W. Cook (1966). The phenomenon of rock splitting parallel to the direction of maximum compression in the neighbourhood of a surface. Proc. 1st Congr. Int. Soc. Rock. Mech., Lisbon, 1, 687-692.

Hoek, E., and Z. T. Bieniawski (1965). Brittle fracture propagation in rock under compression. Int. J. Fract. Mech., 1, 137-155.

Holzhausen, C. R., and A. M. Johnson (1979). Analyses of longitudinal splitting of uniaxially compressed rock cylinder. Int. J. Rock Mech. Min. Sci. & Geomech. Abstr., 16, 163-177.

Horii, H., and S. Nemat-Nasser (1983). Compression-induced micro-crack growth in brittle solids: axial splitting and shear failure; submitted to J. Geophys. Res..

Janach, W. (1977). Failure of granite under compression. Int. J. Rock Mech. Min. Sci. & Geomech. Abstr., 14, 209-215.

Mogi, K. (1966). Pressure dependence of rock strength and transition from brittle fracture to ductile flow. Bull. Earthquake Res. Inst., 44, 215-232.

Murrell, S. A. F. (1965). The effect of triaxial stress systems on the strength of rocks at atmospheric temperatures. Geophys. J. Roy. Astr. Soc., 10, 231-281.

Nemat-Nasser, S. (1983). Non-coplanar crack growth. Proc. ICF Int. Symp. on Fract. Mech., Beijing, China, Nov. 22-26, 185-197.

Nemat-Nasser, S., and H. Horii (1982). Compression-induced nonplanar crack extension with application to splitting, exfoliation, and rockburst. J. Geophys. Res., 87(B8), 6805-6821.

Nemat-Nasser, S., and H. Horii (1983). Rock failure in compression; to appear in Int. J. Engrg Sci./Letters in Appl. & Engrg Sci. (in press).

Olsson, W. A., and S. S. Peng (1976). Microcrack nucleation in marble. Int. J. Rock Mech. Min. Sci. & Geomech. Abstr., 13, 53-59.

Paterson, M. S. (1978). Experimental Rock Deformation - The Brittle Field. Springer-Verlag, Berlin-Heidelberg-New York.

Peng, S. D., and A. M. Johnson (1972). Crack growth and faulting in cylindrical specimens of Chelmsford granite. Int. J. Rock Mech. Min. Sci., 9, 37-86.

Tapponnier, P., and W. F. Brace (1976). Development of stress-induced microcracks in Westerly granite. Int. J. Rock Mech. Min. Sci. & Geomech. Abstr., 13, 103-112.

Wong, T. F. (1982). Micromechanics of faulting in Westerly granite. Int. J. Rock Mech. Min. Sci. & Geomech. Abstr., 19, 49-64.